PERFORMANCE ANALYSIS OF INTEGRATION OF SOLAR PV-WECS AND DG SET FOR AN EV CHARGING STATION BASED ON AN ANFIS CONTROLLER

THOTA PRAVEEN KUMAR[1] VISHWANALA ANJANI KUMAR[2] NIMMALA THIRUMALA[3] EEGA PRAVEEN[4] CHITTETI SAKETH REDDY[5]

[1]Associate Professor & head, Department of EEE, Jyothishmathi institute of technology and science, Nustulapur, Karimnagar, T.S, India.

[2,3,4,5]UG students, Department of EEE, Jyothishmathi institute of technology and science, Nustulapur, Karimnagar, T.S., India

praveen.t@jits.ac.in , anjanikumar0304@gmail.com , thirumalanimmala77@gmail.com , eegapraveen2004@gmail.com , nanisaketh868@gmail.com

Abstract: A solar PV-WECS and diesel generator based electric vehicle charging station is Primary objective of this project. Continuous loading of isolated, grid-connected, and DG-connect modes is achieved in this study via Cues of photovoltaic (PV) panels, a wind energy conversion system (WECS), a diesel generator (DG), and a grid-based electric vehicle charging station (CS).In order to manage Voltage and frequency, this project switches out CVPI controller in CVDG set with an ANFIS controller. In both isolated and grid or DG set linked modes, charging station may supply local household loads with energy from photovoltaic arrays and wind energy conversion systems (WECS). Achieving unity power factor (UPF) functioning of CVGI or a DG set requires Charging station to adjust for Clonal reactive power and harmonics current demand while feeding residential loads and charging electric vehicles. Furthermore, this study takes into account a number of supplementary charging station characteristics, including a vehicle-to-home and vehicle-to-grid connection, harmonics removal, reactive power compensation from Vehicle-to-grid, and synchronization capabilities.

Key terms: charge station, photovoltaic, electric car, power quality, wind energy conversion system, and adaptive neurofuzzy inference controller.

I.INTRODUCTION

Current global pollution crisis is being caused by automobiles powered by fossil fuels, and many are turning to electric vehicles (EVs) as a solution. In addition, EVs may be Answer to this issue [1]- [2]. Since fossil fuels still account for Cast majority of World's electrical output, many people are sceptical that electric vehicles can alleviate pollution and Scarcity of these resources. Hence, a lot of academics have proposed charging EVs using renewable energy. A method for Sizing of CVPV array for Fully green charging system was published by Ugirumurera et al. [3]. A rapid charging method for electric vehicles powered by photovoltaic arrays was created by Good et al. [4]. Three-port configuration for PV array and EV integration has been experimentally proven by Gambia et al. [5]. Impact of integrating a storage battery into CVPV charging station (CS) has been investigated by Chaudhary et al. [6]. CVPV array, according to Liu et al. [7], is well-suited for EV CS that makes use of Commercial building's on-site produced electricity. Cues of PV panels over parking lots has been supported by Zhang et al. [8]. In order to lessen Impact of power fluctuations in utilities that generate wind power, Tawakoni et al. [9] used Electric vehicle battery. Renewable energy-supported CS has Ability to reduce CVGI's impact from EV charging and satisfy Crowing demand for charging, according to Coexisting research. Nevertheless, Majority of Published works mostly deal with theoretical investigations, such as how to maximize Size of various renewable energy sources using charging patterns, sun irradiance, and wind pattern of speeds [10]. Charging schedule of electric vehicles has been Subject of several optimization methods with Coal of making Coast efficient use of renewable energy sources [11]- [12]. In an effort to keep charging costs down, Economics of Charging station have been Subject of many articles [13]. Both Utility and CVEV user may profit from Auxiliary services provided by EVs, according to certain studies [14]. Having said that, Installation of charging stations has been covered by very few publications. It is crucial to monitor and build

Charging station for real application since electric vehicle charging uses several energy sources with varying characteristics. In light of Fact that PV array and WECS power production disruptions are addressed in this study, Implementation of CS is detailed. In addition, CVCS employs DG set in conjunction with grid for backup charging. These are Primary benefits that CVCS has brought about. Constructing an electric vehicle charging station and a local household load backup power system via Integration of many energy sources. Create a control technique that uses many energy sources sequentially or all at once to charge electric vehicles continuously. Charging station's control approach should be designed to accommodate its multimode functioning. Carious operating modes of CVCS are compliant with IEEE standards. Plans for maximizing Efficiency of CVPV system and Wind energy conversion system. Develop a plan to load CVDG set as efficiently as possible.

II. EXISTING SYSTEM

Current approach just addresses CV GI-connected or island-based modes when discussing Performance of CS. Although solar irradiance is present, Collar PV panel becomes useless in Cement that CVGI goes down because of Single mode of operation in grid linked mode. Intermittent nature of solar radiation also disrupts PV power in island mode. Consequently, a storage battery is necessary to reduce Impact of fluctuating solar irradiation. To prevent Storage battery from being overcharged, it is necessary to disengage Maximum Power Point Tracking (MPPT) after Cattery is completely charged. Using Current PI controller IV, following figure demonstrates Vinified control of CVVSC in both standalone and grid and DG set linked modes.

III. SUGGESTED SYSTEM

Figure 1 depicts Circuit of Integrated charging station (CS) that has been suggested. Charging station, which supplies power to both EVs and backup power to local household loads, is built using an integrated PV array, brushless permanent magnet generator (PMBLDC) based WECS (Wind Energy Conversion System), and diesel generator (DG) set. CVDC link and CVCS's point of common coupling (PCC) are connected by an insulated gate bi-polar junction transistor (IGBT) based converter. Power is transferred at CVDC link by CVPV array and WECS using boost converters, while power is exchanged at CVPCC by CVDG set and CVGI. Electric vehicle also uses a bidirectional DC-DC converter to get power from CVDC connection. Electric vehicle can transmit electricity in both directions, from CVGI to Residence, thanks to Bidirectional converter. An active switch with two-way power transfer capabilities connects CVGI and CVDG set to CVPCC. Power is also drawn from CVPCC by Clonal residential loads. In landed and DG set or grid linked modes, switching noise is filtered by placing an RC filter on both sides of Cato-way switch.

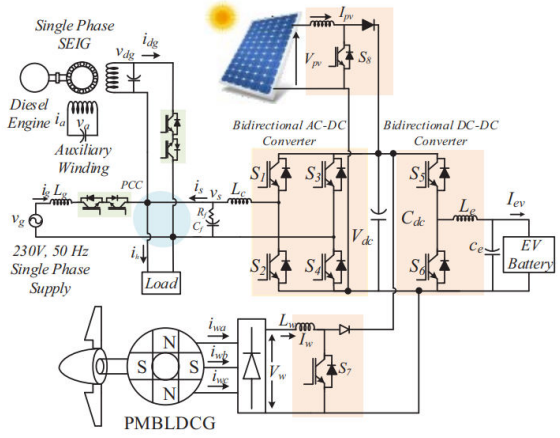

Fig. 1 Topology of charging station

IV CONTROL STRATEGIES

According to Charging station's operation strategy (Fig. 2), Castration combines several energy sources and runs in various modes to continually charge Electric vehicle. Thus, Control system must be designed to maximize Cues of all energy sources while ensuring that charging of electric vehicles and Supply of residential loads are not negatively impacted. On top of that, charging station must be able to handle many modes of operation and different power quality standards. Hence, isolated mode, grid connected mode, and DG set connected mode control designs are covered. Controller's job in island mode is to manage CVDC link voltage (Vac) and produce a sinusoidal voltage (vs) at PCC. Figure 5 shows Control loop in action, which generates Voltage by comparing Reference current (I * s) with Victual PCC voltage (vs). Hysteresis controller generates CVVSC's gating pulses based on Current error (vase), as seen in Figure 5. Alternating between island and grid-connected modes is another function of Islanded control. Accordingly, Controller in Figure 3 determines Corrected phase (am) for CVVSC operation by acquiring Chase angles of CVGI voltage (Mg) and

CVPCC voltage (Is). At PCC, adjusted voltage is created using Corrected phase. By providing Electric vehicles and loads' reactive power demands and harmonic currents locally, Controller may ensure that active power is used only in grid or DG set linked mode, without compromising power quality.

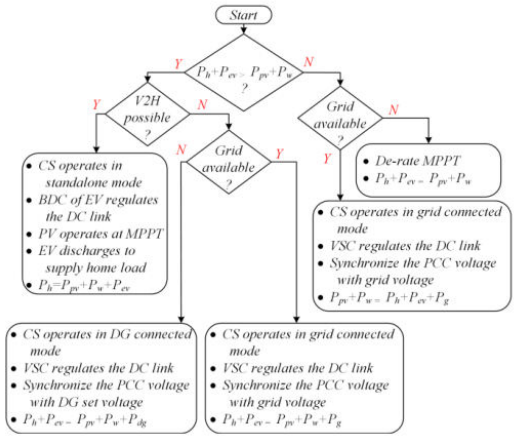

Fig. 2 Strategy for Cooperation of CS

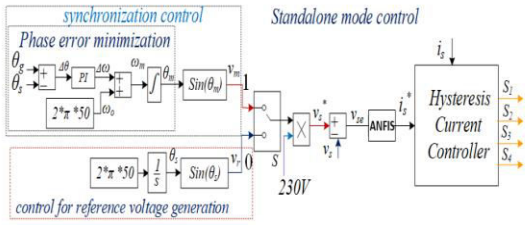

Fig. 3 Control diagram in standalone mode

Figure 4 shows Control diagram for Commode that is linked to CVGI or DG sets. This is accomplished by estimating Sinusoidal reference current (I * g) in phase with CVGI voltage (vg) by use of Amplitude adaptive notch filter (AANF) [15]. Cave, ′Y, and μ parameters determine CVAANF algorithm's performance. Actual positive parameters that may be adjusted are B, ζ, and μ. ζ and γ dictate how fast CVAANF converges and how accurate its estimates are. Caveating signals for CVVSC are provided by Hysteresis controller using either Reference grid (I * g) or CVDG set current (I * dg). Similar to CVGI-connected controller, CVDG-connected controller lacks a voltage and frequency regulation loop, but otherwise functions similarly. Output of these loops stays at zero when they are connected to CVGI. Two cascaded PI controllers are used to regulate CVDC bus voltage in an island state, as shown in Fig. 5. CVDC link voltage and current loop reference are both controlled by Cooter PI controller. To determine Bidirectional converter's duty cycle, CVPI controller reduces Current error as much as possible. When charging electric vehicles in grid-connected mode, a cascade PI control is used (Fig. 6). As a reference for Coiner loop's current estimation, Cooter loop regulates CVEV battery's voltage. As an alternative, Electric vehicle's charging current is controlled by Current loop. Thus, CC charging of CVEV is accomplished for a completely drained EV battery. Upon reaching 80% battery capacity, CVEV's charging system switches to CV mode.

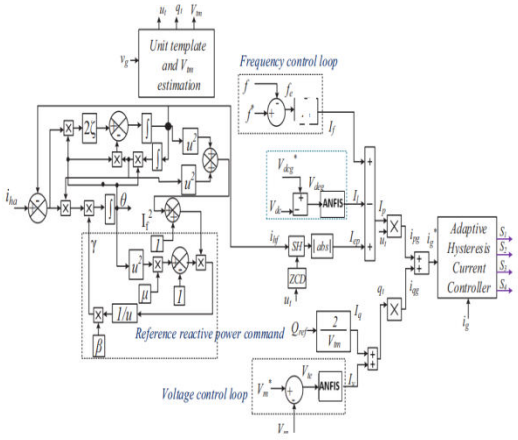

Fig. 4 Control diagram in grid or DG set connected mode

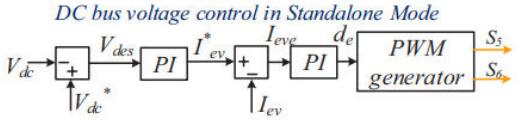

Fig. 5 Strategy for DC link voltage regulation in standalone mode

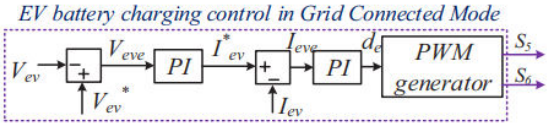

Fig. 6 EV battery control in grid connected mode

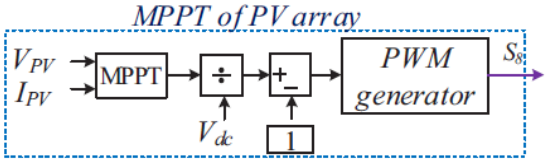

Fig.7 MPPT scheme of Collar PV array

Fig.8 MPPT scheme of WECS

Figure 7 shows Incremental conductance (INC) [16] based maximum power point tracking (MPPT) technique that is used to accomplish MPPT of CVPV

array. CVINC algorithm is used by Controller to estimate CVMPP voltage using voltage and current samples taken from CVPV array. An estimate of Boost converter duty cycle is made using Voltage at MPP and CVDC link voltage. CVINC-based MPPT method is also used to extract Maximum power of WECS. Figure 8 shows Control diagram for CVMPPT

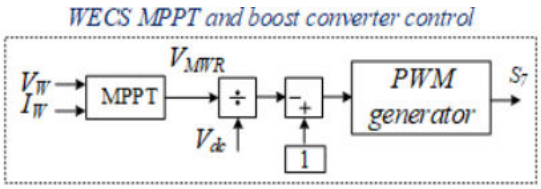

control of CVWECS. As mentioned before, Maximum power extraction technique is comparable to Collar PV array MPPT.

V. PROPOSED ANFIS CONTROLLER

Another name for ANFIS is neuro-fuzzy adaptive inference system. Fuzzy logic and neural networks are both included into it. Inputs determine how many inputs are transmitted through Neural network. Neural network is trained using its performance and inputs. Fuzzy logic is used to include performance after neural network training. Cruces and membership functions are generated via fuzzy logic. Figure 9 below shows CVANFIS design.

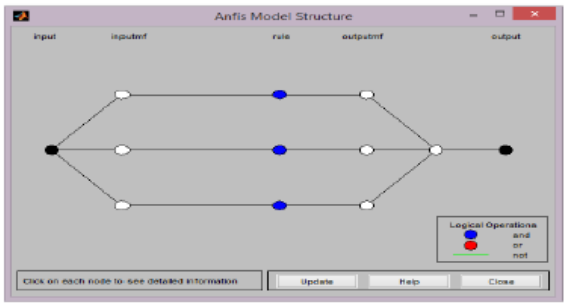

Fig. 9 ANFIS architecture

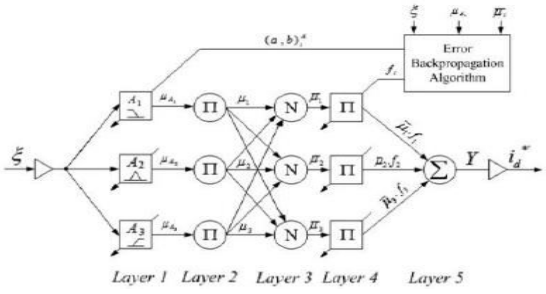

Fig 10 Schematic of Proposed ANFIS

Neurofuzzy controller will make an error when it compares Creel DC-link voltage to Civic-link reference value. (ξ = Vac*-Vac), Precondition and following parameters will also be impacted by a comparable error. Calculation of Captive current injected into RES (Iren) is done using Captive current (id*') component of Civic-link voltage controller. **Layer 1:** Its name, Primary Level, Things begin to become murky at this point. Membership degree of each input variable is calculated in this layer. An ANFIS input variable is error (e) and an error change (e). To reduce measurement error, as shown in Figure 11, trapezoidal and triangle registration capabilities are used. Requirements for nodes are, as will be detailed below: c_i

$$O_{1i} = \mu\_A_i(x) = \frac{1}{1+\left(\frac{x-ci}{ai}\right)^{2bi}} \qquad i=1,2,3 \qquad (1)$$

Following is a definition of premise parameters: x is Coventry for Node-I, Ai is Associated linguistic variable, and bi, ci is Collection of premise parameters.

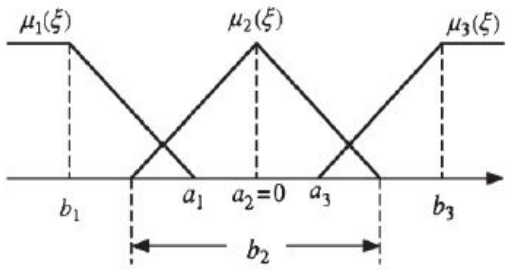

Fig.11 Fuzzy membership functions.

Layer 2: Its name, CV"inferior" layer refers to Second level of Crenulation. Input is multiplied and Output is sent out by each fixed node in this layer. Each node's firing intensity represents its energy consumption according to a fuzzy rule.

$$O_{2i} = \mu_i = \mu_{Ai}(x).\mu_{Bi}(y) \qquad i=1,2,3 \qquad (2)$$

Layer 3: Its name, Normalising layer, says it all. Around each node in a layer is an N-labelled circular node. Firing force ratio according to Crenulations is determined at Civet node.

$$O_{3i} = \mu_i = \frac{\mu i}{\mu 1+\mu 2+\mu 3} \qquad i=1,2,3 \qquad (3)$$

Layer 4: It's Final product, Functionality and adaptable mode is available on all nodes.

$$O_{4i} = \mu_i.f_i = \mu_i(a_{0i}+a_{1i}\epsilon) \quad i=1,2,3 \quad (4)$$

Resulting parameter set where Output of Layer 3 is with (a_0, a_1).

Layer 5: As Came implies, here is where Data is sent out to Outside world. In this layer, there is just one node, which is Cesium of all Input signals, and it is labelled as,

$$O_{5i} = \mu_i = \sum_{i=1}^{N} \mu i.\, fi \quad i=1,2,3 \quad (5)$$

Errors in Back propagation of CVANFIS parameters are corrected,

$$\frac{\partial E}{\partial O5} = k_1.e + k_2.\Delta e \quad (6)$$

CV k_1 and k_2 coefficients are multiplied to get error (e) and Change in error (Δe).

$$\alpha_{k+1} = \alpha_k - \eta\frac{\partial E}{\partial \alpha k} \quad (7)$$

When a certain ANFIS parameter is updated, the learning rate is applied, and the error is incorporated into the following round of training.

VI. SIMULATION RESULTS

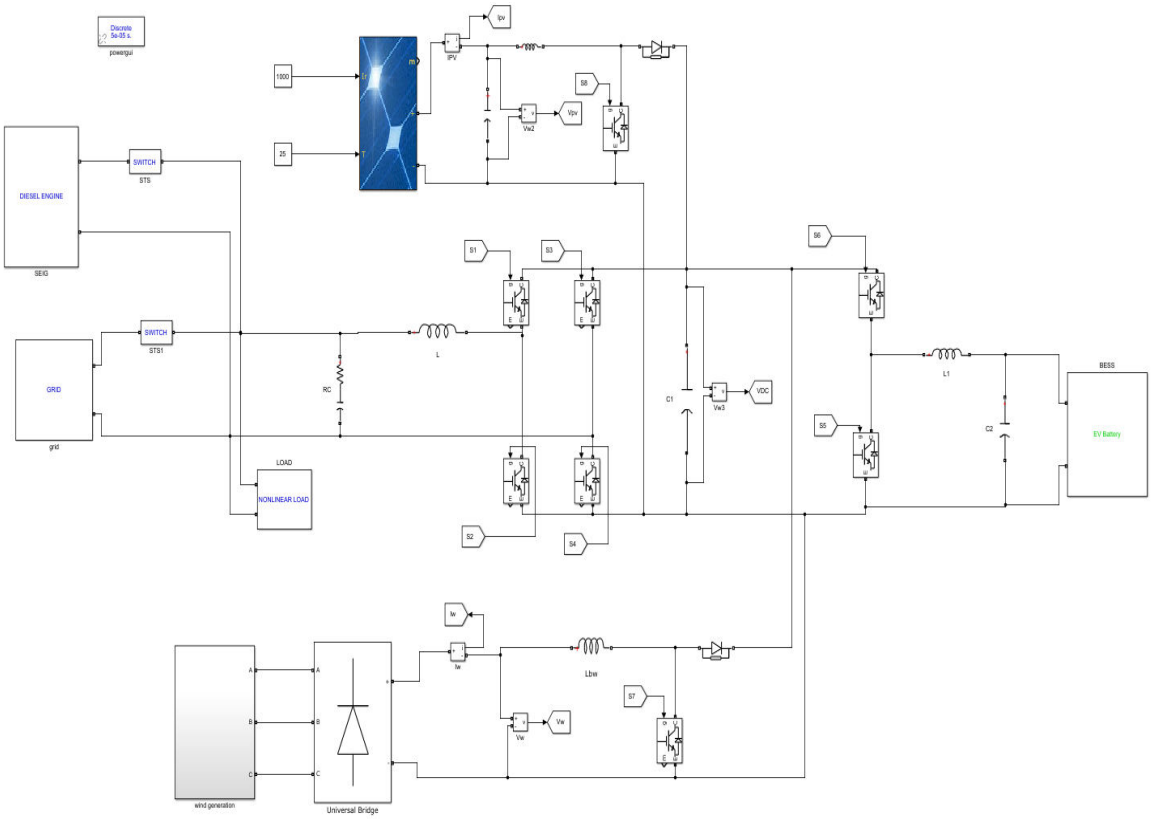

Fig 12. MATLAB/SIMULINK circuit of System

A) EXISTING RESULTS

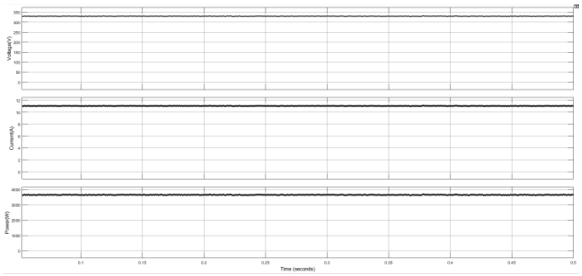

(a)

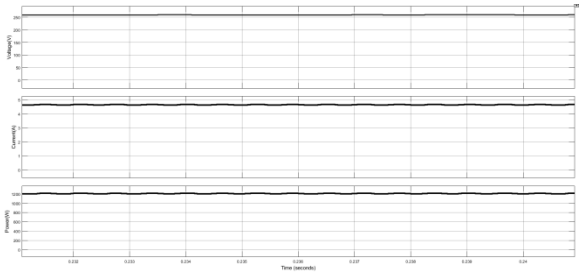

(b)

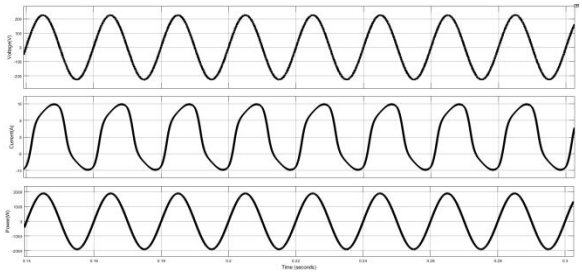

(c)

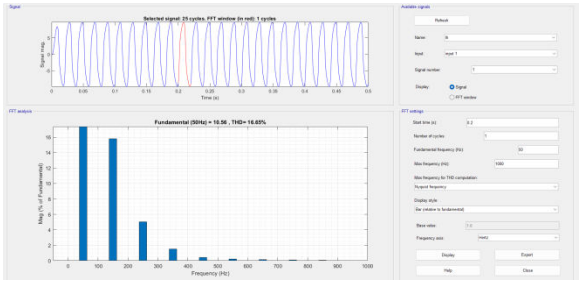

(d)

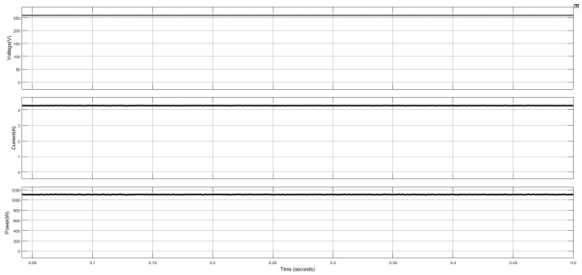

(e)

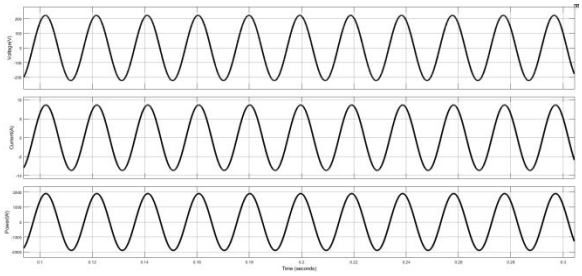

(f)

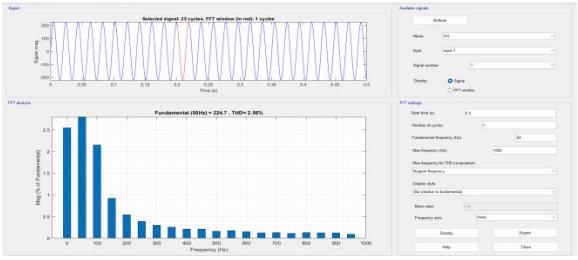

(g)

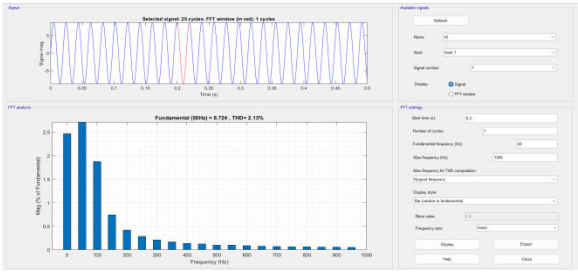

(h)

Fig. 13 Steady state performance in grid connected mode, (a) V_{pv}, I_{pv}, and P_{pv}, (b) V_w, I_w, and P_w, (c) v_c, i_h, and P_h, (d) harmonic spectrum of i_h, (e) V_b, I_b, and P_b, (f) v_g, i_g, and P_g, (g)-(h) harmonic spectra of v_g and i_g

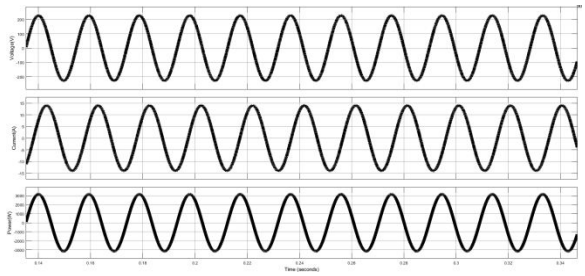

(a)

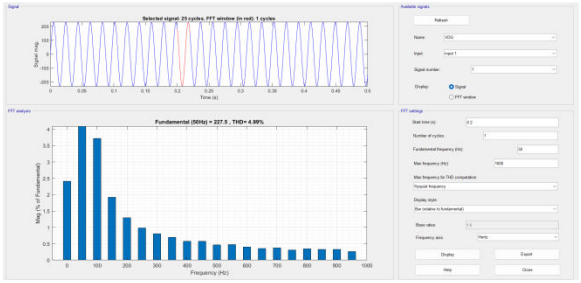

(b)

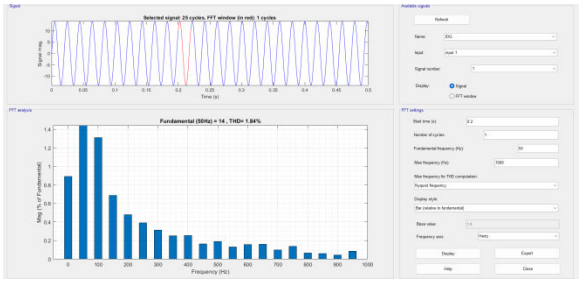

(c)

Fig.14 Performance of DG set in DG set connected mode, (a) v_{dg} and i_{dg} and DG set power, (b)-(c) harmonic spectrum of i_{dg} and v_{dg}

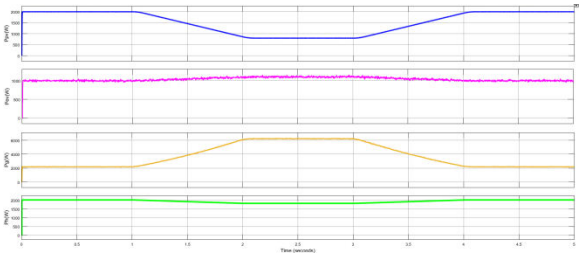

(a)

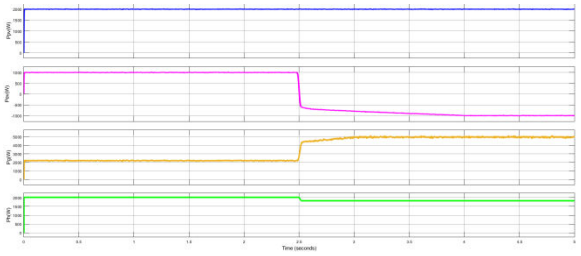

(b)

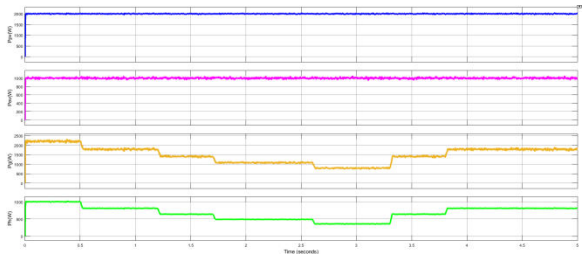

(c)

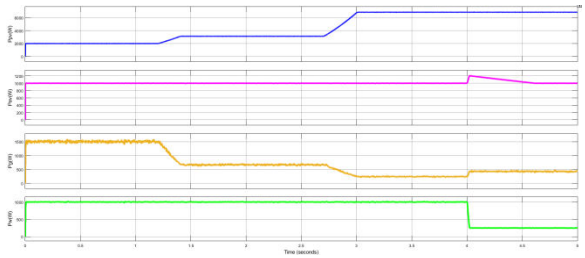

(d)

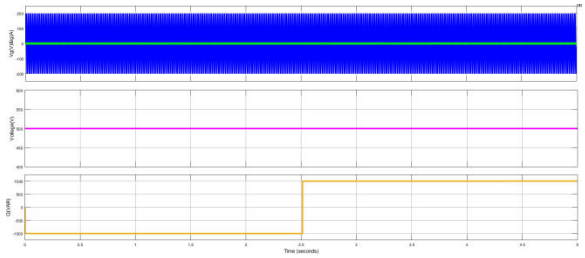

(e)

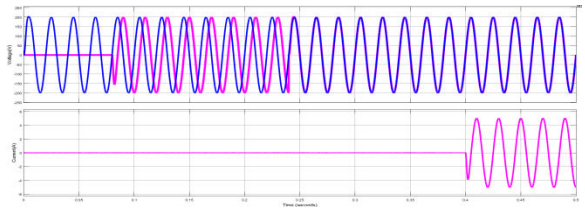

(f)

Fig. 15 Behavior in grid tied condition, (a) under Disturbance in irradiance power level, (b) EV (Vehicle-to-grid) mode change, (c) under Change in household load, (d) under Change in WECS power generation, (e) load reactive power compensation, (f) grid connection and disconnection.

(a)

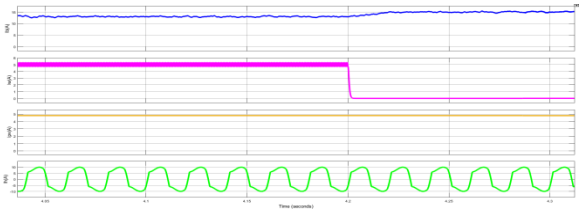

(b)

Fig. 16 Dynamic behavior in islanded mode, (a)-(b) vehicle-to-home operation under Change in PV and WECS generated power

B) EXTENSION RESULTS

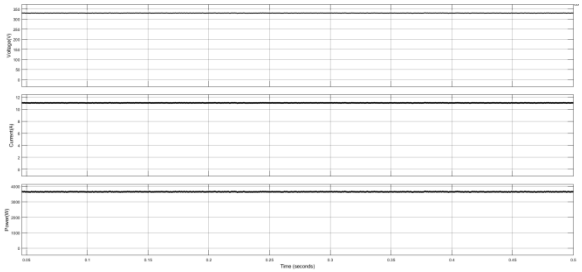

(a)

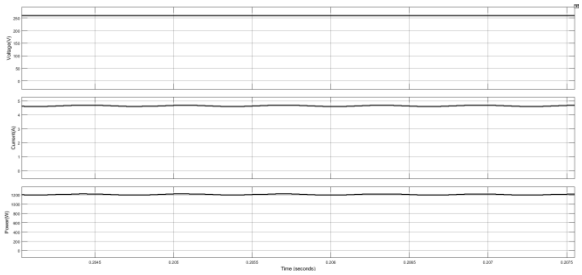

(b)

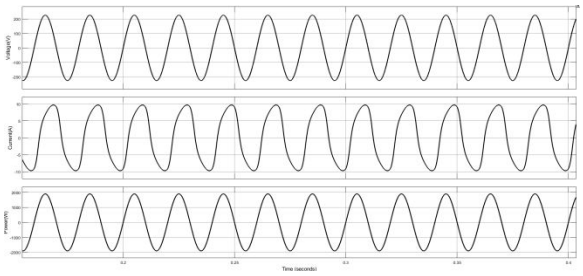

(c)

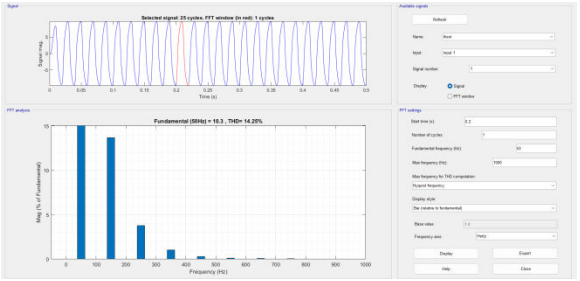

(d)

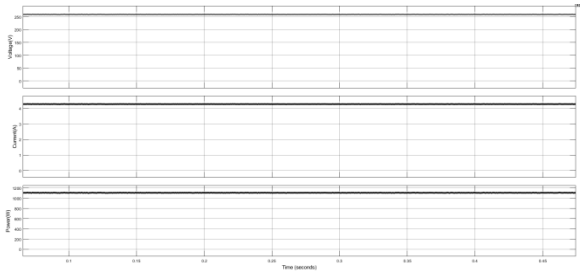

(e)

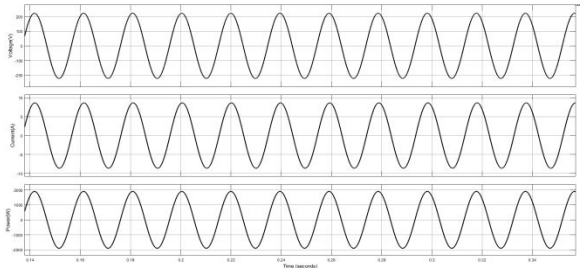

(f)

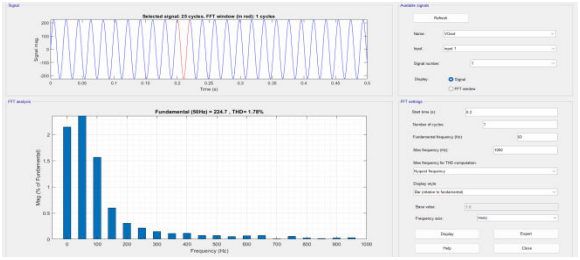

(g)

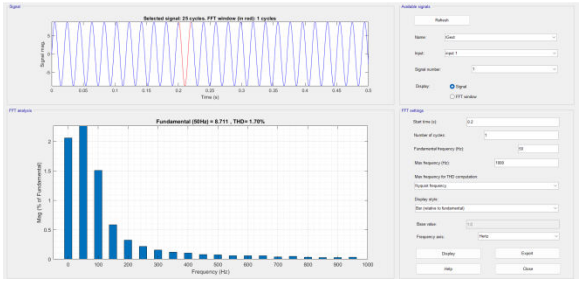

(h)

Fig. 17 Steady state performance in grid connected mode, (a) V_{pv}, I_{pv}, and P_{pv}, (b) V_w, I_w, and P_w, (c) v_c, i_h, and P_h, (d) harmonic spectrum of i_h, (e) V_b, I_b, and P_b, (f) v_g, i_g, and P_g, (g)-(h) harmonic spectra of v_g and i_g

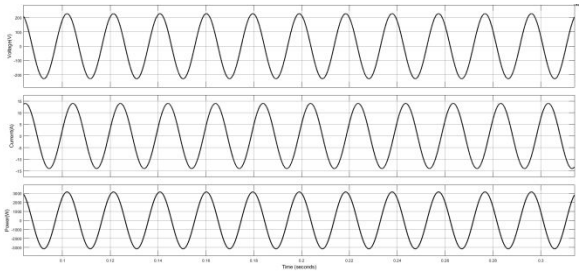

(a)

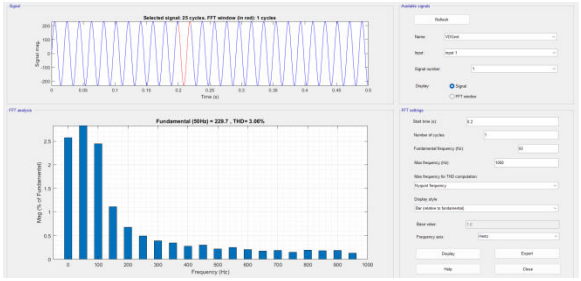

(b)

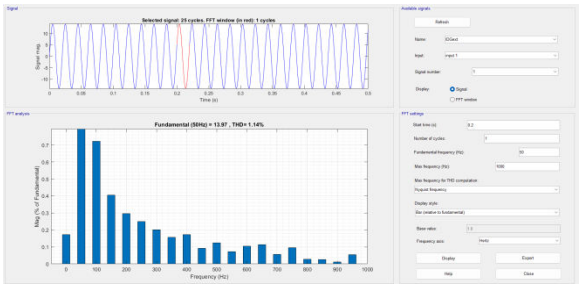

(c)

Fig. 18 Performance of DG set in DG set connected mode, (a) v_{dg} and i_{dg} and DG set power, (b)-(c) harmonic spectrum of i_{dg} and v_{dg}

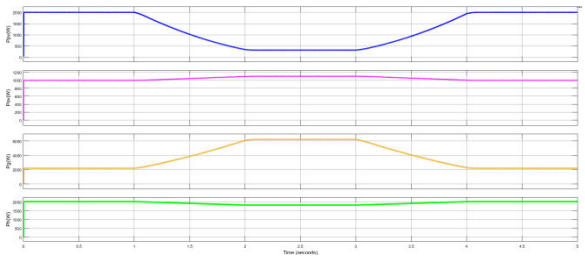

(a)

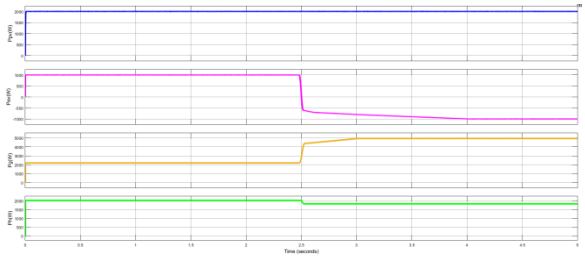

(b)

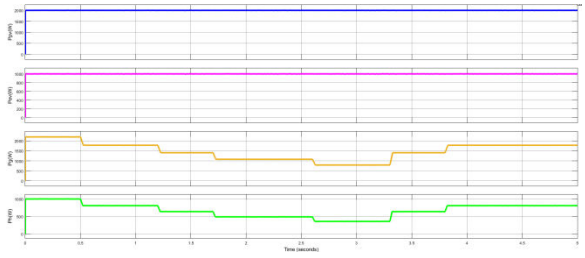

(c)

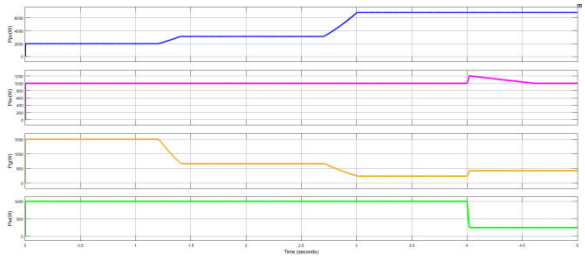

(d)

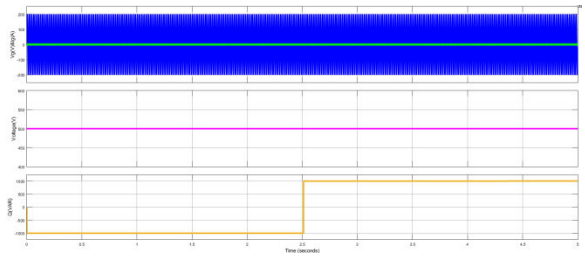

(e)

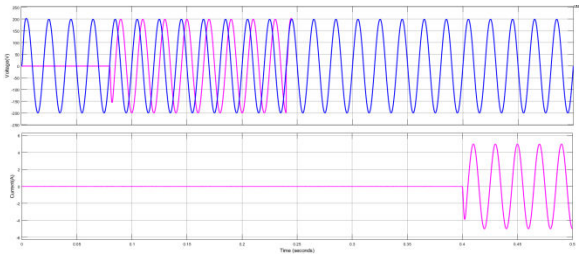

(f)

Fig. 19 Behavior in grid tied condition, (a) under Disturbance in irradiance power level, (b) EV (Vehicle-to-grid) mode change, (c) under Change in household load, (d) under Change in WECS power generation, (e) load reactive power compensation, (f) grid connection and disconnection.

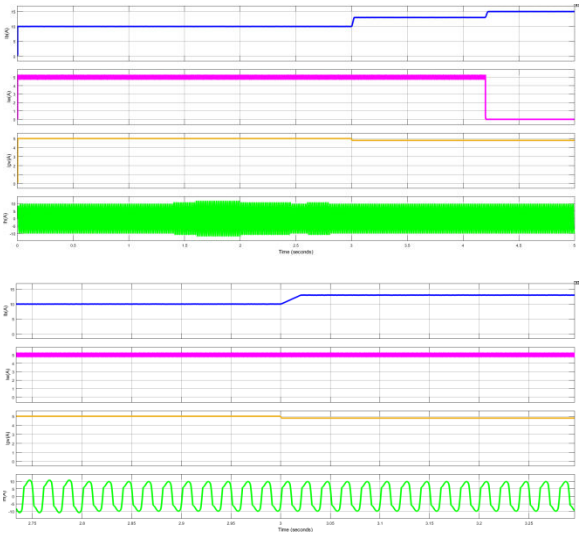

(a)

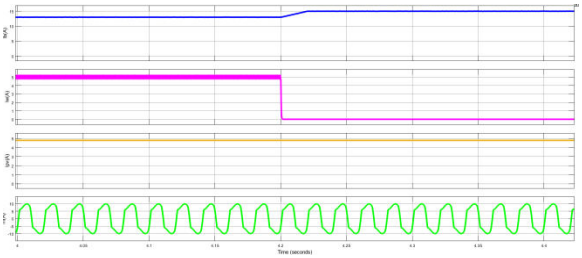

(b)

Fig. 20 Dynamic behavior in islanded mode, (a)-(b) vehicle-to-home operation under Change in PV and WECS generated power

Tabel-1 COMPARISION TABLE

	Existing System	Extension System
Load Current THD%	16.65%	14.25%
Grid Voltage THD%	2.56%	1.78%
Grid Current THD%	2.13%	1.70%
DG set Voltage THD%	4.99%	3.06%
DG set Current THD%	1.84%	1.14%

CONCLUSION

Project's goal is to build a charging station for electric vehicles that makes use of photovoltaic (PV) arrays, wind energy conversion systems (WECS), CVGI, and DG sets. With only one VSC, Findings have shown that CVCS can operate in three modes: island operation, grid connected, and DG set connected. Findings that were given prove that Charging station may function as an independent generator with high voltage quality. CVANFIS controller, automated mode switching, grid connected, and DG set connected operations, as well as Islanded operation, have improved charging reliability, maximized CVPV array's MPP operating probability, and optimized CVDG set's loading. According to table 6.1, Suggested ANFIS controller results in lower THD when compared to CVPI controller and CVTHD compassion table. There are several supplementary functions of Charging station that have been validated by Provided findings. These include Capacity to synchronize, eliminate harmonics, compensate reactive electricity from vehicles to CVGI, and connect vehicles to homes.

REFERENCES

[1] International Energy Agency-Global EV Outlook 2018- Towards cross-modal electrification. [Online] Available:*https://webstore.iea.org*/download/direct/1045? fileName=Global_EV_Outlook_2018.pdf

[2] International Energy Agency- Renewables 2O18 - Analysis and Forecasts to 2O23 [Online]. Available: https://webstore.iea.org/ download/summary/2312? fileName=English-Renewables-2018ES.pdf.

[3] J. Ugirumurera and Z. J. Haas, “Optimal Capacity Sizing for Completely Green Charging Systems for Electric Vehicles,” IEEE Trans. Transport at. Electrificat.vol. 3, no. 3, pp. 565-577, Sept. 2017.

[4] G. R. Chandra Moulid, J. Schijffelen, M. van den Heave, M. Carolus and P. Bauer, “A 10 kW Solar-Powered Bidirectional EV Charger Compatible with Chemo and COMBO,” IEEE Trans, Power Electron., vol. 34, no. 2, pp. 1082-1098, Feb. 2019.

[5] V. Monteiro, J. G. Pinto and J. L. Alonso, “Experimental Validation of a Three-Port Integrated Topology to Interface Electric Vehicles and Renewables with Electrical Grid,” IEEE Trans. Ind. Informant., vol. 14, no. 6, pp. 2364-2374, June 2018.

[6] S. A. Singh, G. Carli, N. A. Aziz and S. S. Williamson, “Modeling, Design, Control, and Implementation of a Modified Z-Source Integrated PV/Grid/EV DC Charger/Inverter,” IEEE Trans. Ind. Electron., vol. 65, no. 6, pp. 5213-5220, June 2018.

[7] K. Chaudhary, A. Kill, K. N. Kumar, U. Jalandhar and S. K. Kollimalla, “Hybrid Optimization for Economic Deployment of ESS in PV-Integrated EV Charging Stations,” IEEE Trans. Ind. Informat., vol. 14, no. 1, pp. 106-116, Jan. 2018.

[8] F. Kineavy and M. Duffy, “Modelling and design of electric vehicle charging systems that include on-site renewable energy sources,” in IEEE 5th Int. Sump. Power Electron. For Distributed Gene. Syst. (PEDG), Galway, 2014, pp. 1-8.

[9] Y. Zhang, P. You and L. Cain, “Optimal Charging Scheduling by Pricing for EV Charging Station with Dual Charging Modes,” IEEE Trans. Intelligent Transport at. Syst., vol. 20, no. 9, pp. 3386-3396, Sept. 2019.

[10] Y. Yang, Q. Jian, G. Deconinck, X. Guan, Z. Qi and Z. Hu, “Distributed Coordination of EV Charging with Renewable Energy in a Micro grid of Buildings,” IEEE Trans. Smart Grid, vol. 9, no. 6, pp. 6253-6264, Nov. 2018.

[11] N. K. Kandalama, K. Kandalama and K. J. Tseng, “Loss-of-life investigation of EV batteries used as smart energy storage for commercial building-based solar photovoltaic systems,” IET Electrical Systems in Transportation, vol. 7, no. 3, pp. 223-229, 9 2017.

[12] A. Tawakoni, M. Negnevitsky, D. T. Nguyen and K. M. Mutt qi, “Energy Exchange Between Electric Vehicle Load and Wind Generating Utilities,” IEEE Trans. Power Sys., vol. 31, no. 2, pp. 1248-1258, 2016.

[13] Y. Shan, J. Hu, K. W. Chan, Q. Fu and J. M. Guerrero, “Model Predictive Control of Bidirectional DC-DC Converters and AC/DC Interlinking Converters - A New Control Method for PV-Wind-Battery Micro grids,” IEEE Trans. Sustain. Energy, Early Access.

[14] P. Liu, J. Yu and E. Mohammed, “Decentralized PEV charging coordination to absorb surplus wind energy via stochastically staggered dual-tariff schemes considering feeder-level regulations,” IET Gene., Trans. & District., vol. 12, no. 15, pp. 3655-3665, 28 8 2018.

[15] B. Singh, A. Verme, A. Chandra and K. Al-Haddad, “Implementation of Solar PV-Battery and Diesel Generator Based Electric Vehicle Charging Station,” in IEEE Int. Conf. Power Electronics, Drives and Energy Systems (PEDES), Chennai, India, 2018, pp. 1-6.

[16] N. Sabena, B. Singh and A. L. Vyas, “Integration of solar photovoltaic with battery to single-phase grid,” IET Generation, Transmission & Distribution, vol. 11, no. 8, pp. 2003-2012, 1 6 2017.

[17] H. Rami and H. Doagou-Mojarrad, “Comparative assessment of two different modes multi-objective optimal power management of micro-grid: grid-connected and stand-alone,” IET Renewable Power Generation, vol. 13, no. 6, pp. 802-815, 2019.

[18] O. Erin, N. G. Petrakis, T. D. P. Mendes, A. G. Bakeries and J. P. S. Catalo, “Smart Household Operation Considering Bi-Directional EV and ESS Utilization by Real-Time Pricing-Based DR,” IEEE Trans. Smart Grid, vol. 6, no. 3, pp. 1281-1291, May 2015.

[19] Kumar, T. P., Ganapathy, S., & Manikandan, M. (2024). Voltage stability analysis for grid connected PV system using optimized control on IOT based ANFIS. Przegląd Elektrotechniczny, 100. DOI: 10.15199/48.2024.02.53 .

[20] Thota, P. K., Somaskandan, G., & Mani, M. (2023). The Voltage stability analysis for grid-connected PV system using optimized control tested by IEEE 14 & 30 bus system. Int. J. Exp. Res. Rev,30,

109118.DOI: https://doi.org/10.52756/ijerr.2023.v30.012.

[21] Kumar, T. P., Ganapathy, S., & Manikandan, M. (2022). Improvement of voltage stability for grid connected solar photovoltaic systems using static synchronous compensator with recurrent neural network. Электротехника и электромеханика, (2 (eng)),69-77.Doi:https://doi.org/10.20998/2074-272X.2022.2.10,

[22] CH, S., & IA, C. (2023). Switched Z-Source Boost Converter in Hybrid Renewable Energy System for Grid-Tied Applications. Journal of Electrical Systems, 19(1).

[23] Balakishan, P., Chidambaram, I. A., & Manikandan, M. (2023). Smart fuzzy control based hybrid PV-wind energy generation system. Materials Today: Proceedings, 80, 2929-2936.